Supplementary Information for

Mechanism of INSR clustering with insulin activation and resistance revealed by super-resolution imaging

Hongru Li [a, b], Jinrui Zhang [a], Yan Shi [a], Guanfang Zhao [a, b], Haijiao Xu [a], Mingjun Cai [a, b], Jing Gao [a, *], Hongda Wang [a, b, c *]

[a]State Key Laboratory of Electroanalytical Chemistry, Changchun Institute of Applied Chemistry, Chinese Academy of Sciences, Changchun, Jilin, 130022, P. R. China

[b]University of Science and Technology of China, Hefei, Anhui, 230026, P. R. China

[c]Laboratory for Marine Biology and biotechnology, Qing dao National Laboratory for Marine Science and Technology, Wenhai Road, Aoshanwei, Jimo, Qingdao, Shandong 266237, China

Corresponding author: Jing Gao [a, *], gaojing@ciac.ac.cn;
Hongda Wang [a, b, c *], hdwang@ciac.ac.cn

Email: gaojing@ciac.ac.cn, hdwang@ciac.ac.cn

Fig. S1.

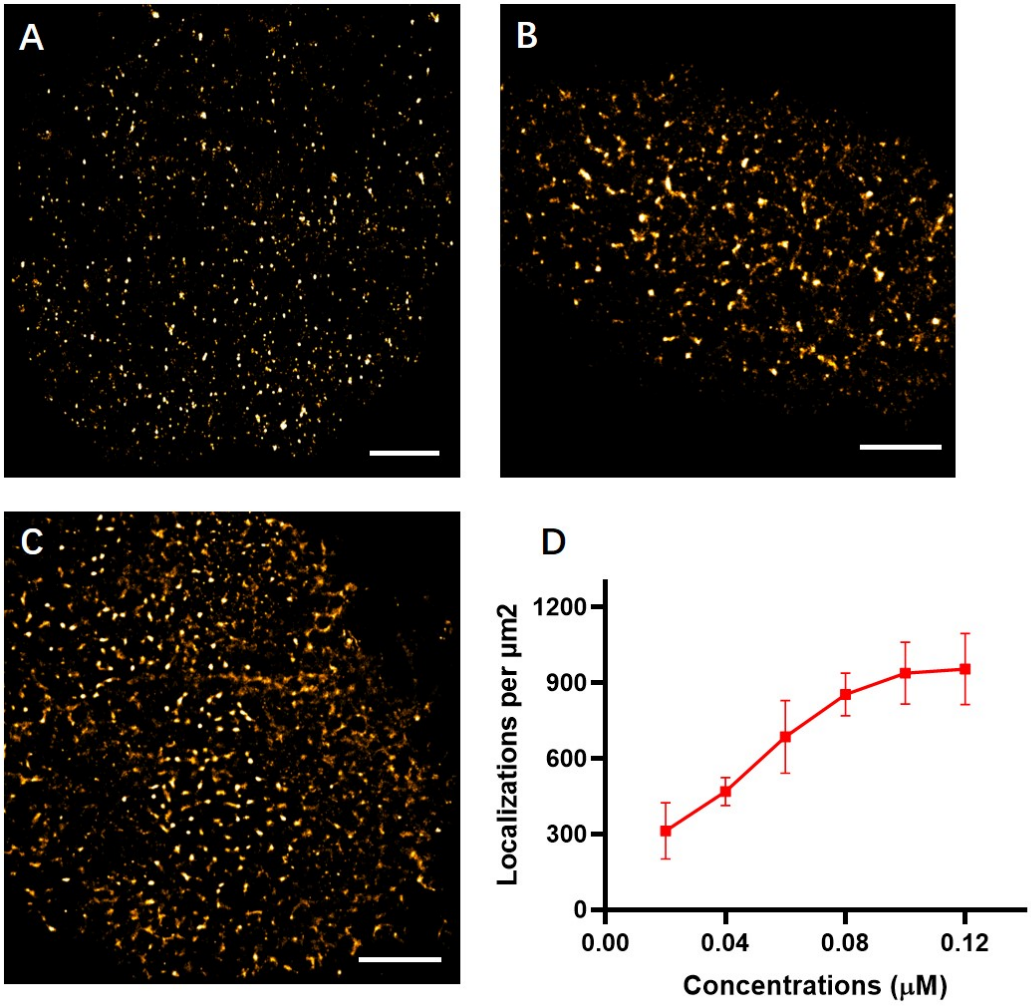

Figure S1. Determination of the labeling concentration of INSR. (A-C), The reconstructed dSTORM images of INSR under the different labeling concentrations of Alexa 532-linked INSR antibody. Scale bar, 4 μm. (A) 0.02 μM, (B) 0.06 μM, (C) 0.1 μM. Scale bars, 4 μm. (D), Variation curve of localization point density with marker concentration. The statistical results were obtained from ten cells in three independent experiments (mean ± SD).

Fig. S2.

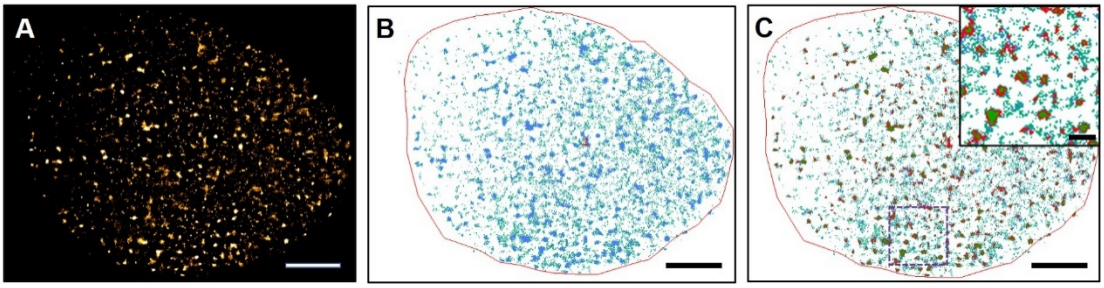

Figure S2. Extraction and analysis of INSR clusters on cell membranes by SR-tesseler method. (A), Reconstructed dSTORM images of INSR on the cell membrane. (B-C), SR-Tesssler extracts clustering maps within the ROI region. Blue represents the objective region, green represents the region of the cluster, and red represents the outline of the cluster. Scale bars, 4 μm (the original images); 400 nm (magnified images).

Fig. S3.

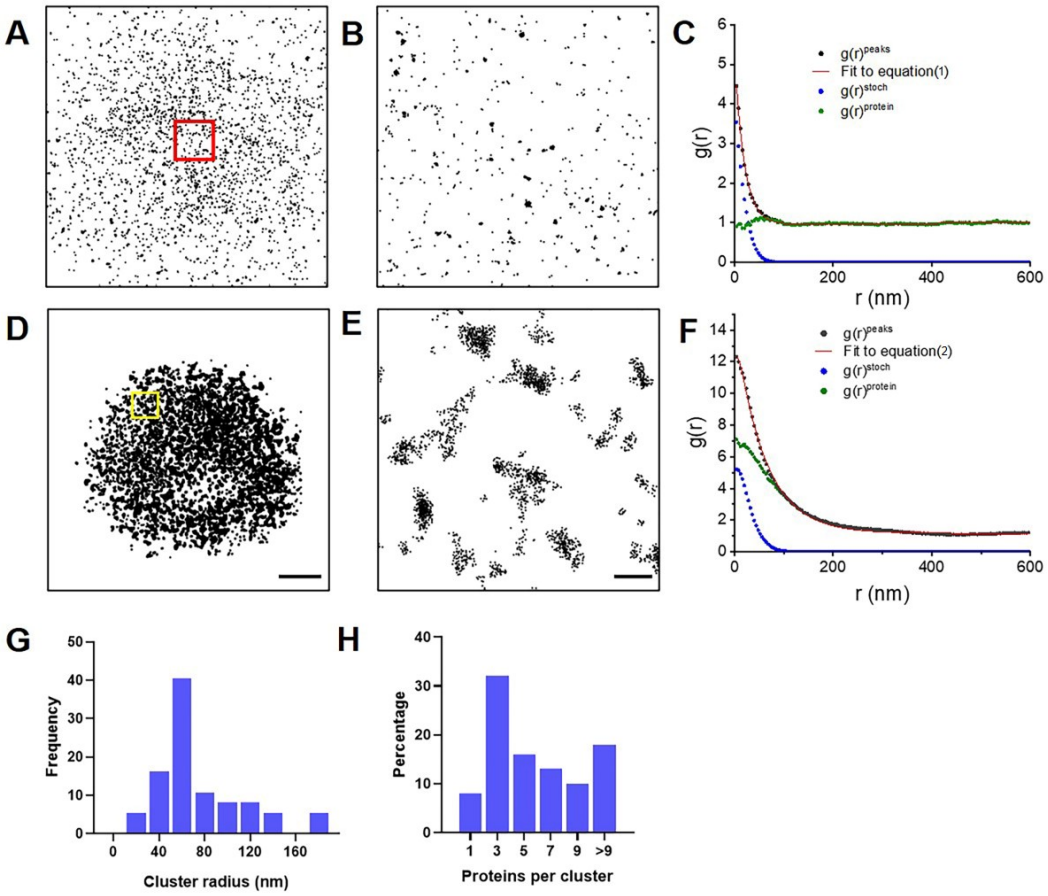

Figure S3. Pair-correlation analysis of insulin receptors on cell membranes. (A), The spatial distribution of Alexa532-linked anti-INSR molecules in a APTES-coverslip. (B), The magnified image of the ROI region in red of A. (C), The plot of calculated auto-correlation function $g(r)^{peaks}$ of Alexa532-linked anti-INSR molecules in B fit to equation (1). The correlation owing to multiple appearances of a single protein $g(r)^{stoch}$ and the protein correlation $g(r)^{protein}$ were evaluated from the fit. (D), The distribution of INSR proteins on the cell membrane. (E), The magnified view of the region in yellow of D. (F), Measured correlation function of all peaks $g(r)^{peaks}$ in E was well fit to equation (2). Corrected protein correlation function $g(r)^{protein}$ was evaluated by subtracting the contribution from multiple appearances of single protein $g(r)^{stoch}$ from the measured correlation function. (G), The percentage of cluster radius. (H), The percentage of clusters containing different proteins. Scale bar, 4μm (A, D), 200nm (B, E).

Fig. S4.

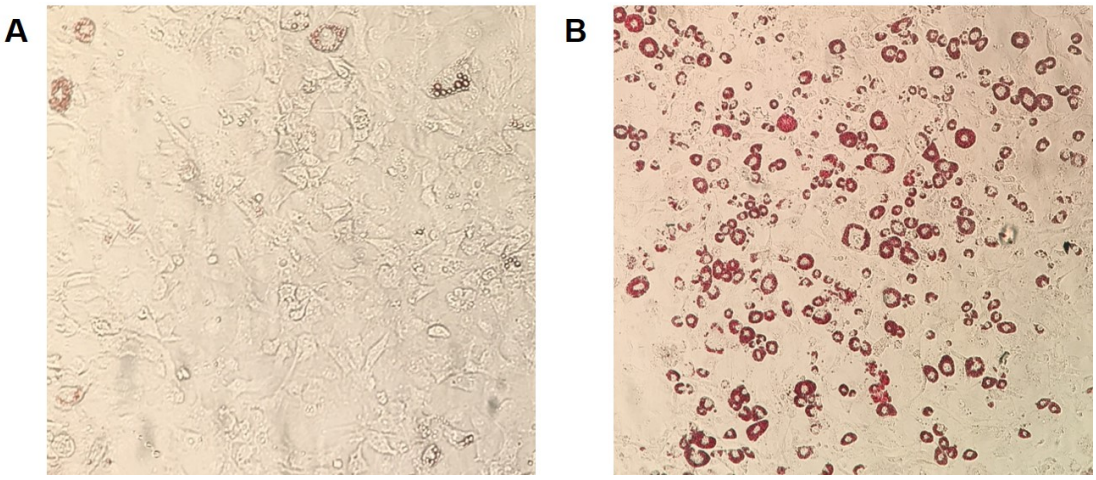

Figure S4. Oil red o staining to verify mature adipocytes. After induction of 3T3-L1 cells by cocktail method, the cells were fixed with 10% PFA for 30 min, stained with oil red o for 10 min, and excess stain was washed off with 75% ethanol, sealed and observed under a 20X microscope. (A), Before oil red o staining. (B), After oil red o staining.

Fig. S5.

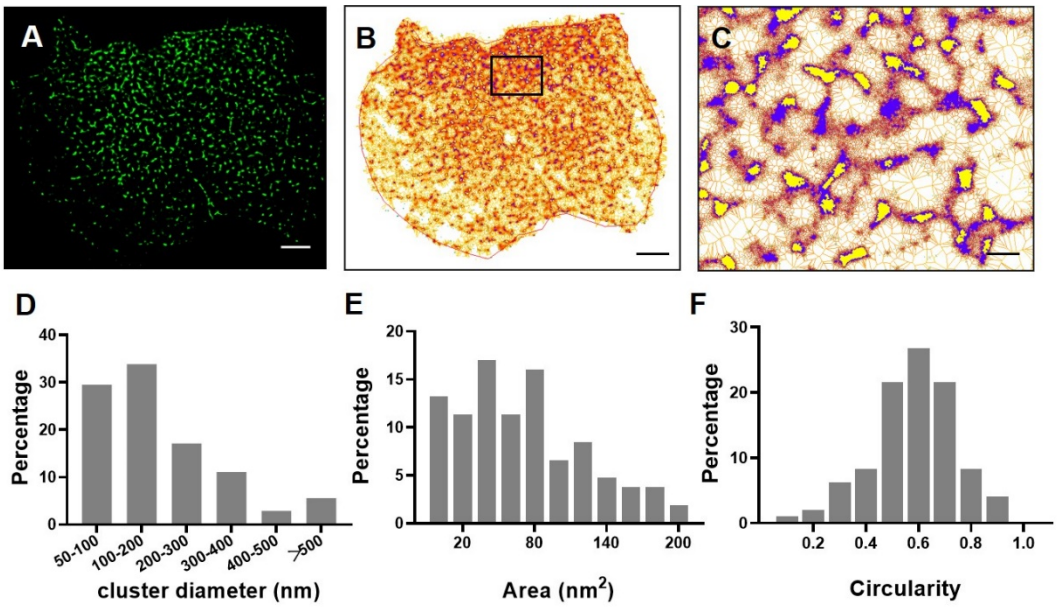

Figure S5. Characterization of βII-spectrin clusters in cell membrane by SR-Tesseler method. (A), dSTORM image of βII-spectrin in cell membrane. (B), corresponding extracted cluster map by SR-Tesseler. (C), Magnified image of the ROI region in B. (D-F), Histogram of different clustering parameters, cluster diameters (D), cluster areas (E), cluster circularity (F). Scale bars, 4 μm (the original images); 400 nm (magnified images).

Fig. S6.

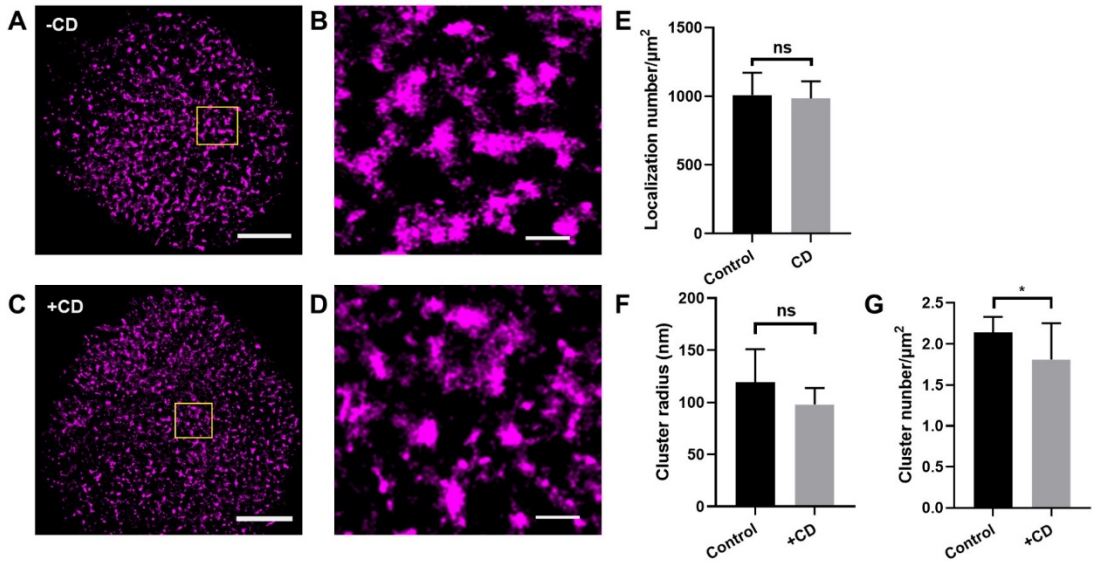

Figure S6. CD treatment does not change the distribution of INSR in the cell membrane. (A–D) Reconstructed dSTORM images of INSR in the cell membrane in control (A) and CD-treated groups (C). (B), Magnified image of the ROI region in A. (D), Magnified image of the ROI region in C. Scale bars, 4 μm (the original images); 400 nm (magnified images). (E), The average number of localizations per μm2. (F), Cluster radius. (G), Cluster number per μm2. The statistical results were obtained from ten cells in three independent experiments (mean ± SD). * p <0.0001, ns. not significant. (Two-tailed unpaired t-test).

Fig. S7.

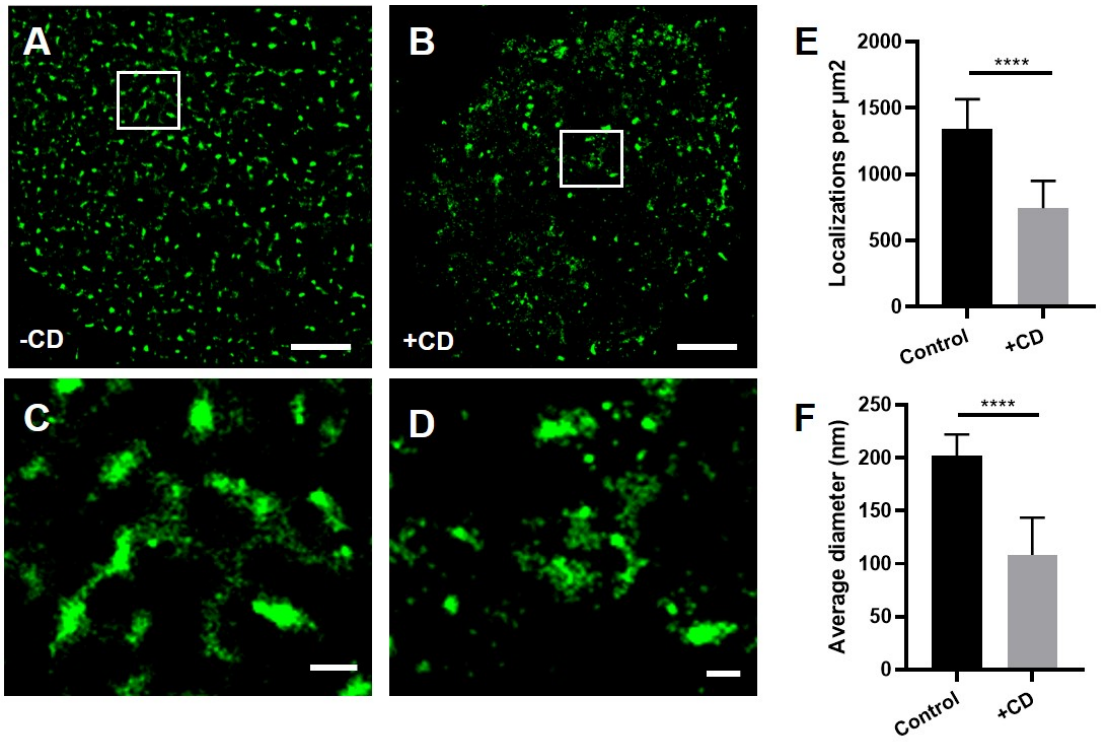

Figure S7. CD treatment disrupts the network structure of βII-spectrin on the cell membrane. (A–D) Reconstructed dSTORM images of βII-spectrin on the cell membrane in control (A) and CytoD-treated groups (B). (C), Magnified image of the ROI region in A. (D), Magnified image of the ROI region in B. Scale bars, 4 μm (the original images); 400 nm (magnified images). (E), The average number of localizations per μm2. (F), The average cluster diameter. The statistical results were obtained from ten cells in three independent experiments (mean ± SD). **** p <0.0001 (Two-tailed unpaired t-test).

Fig. S8.

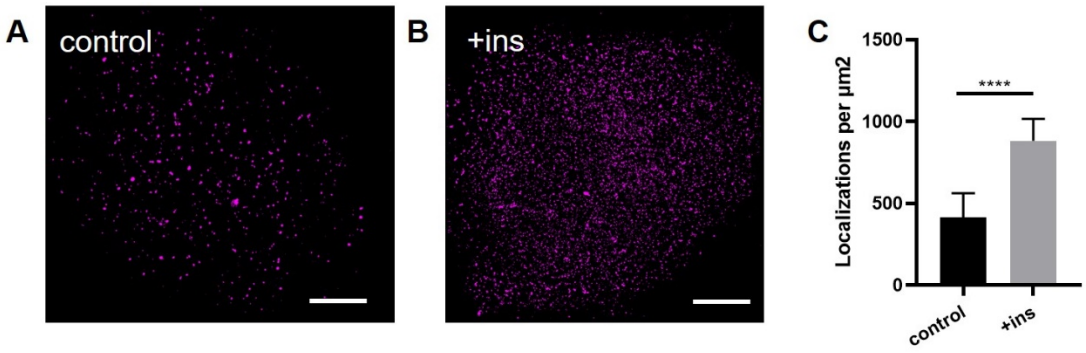

Figure S8. Insulin stimulation leads to GLUT4 aggregation at the cell membrane. (A, B), Reconstructed dSTORM images of GLUT4 on the cell membrane in control (A) and insulin treated groups (B). Scale bars, 4 µm. (C), The average number of localizations per µm2. The statistical results were obtained from ten cells in three independent experiments (mean ± SD). **** p <0.0001 (Two-tailed unpaired t-test).

Fig. S9.

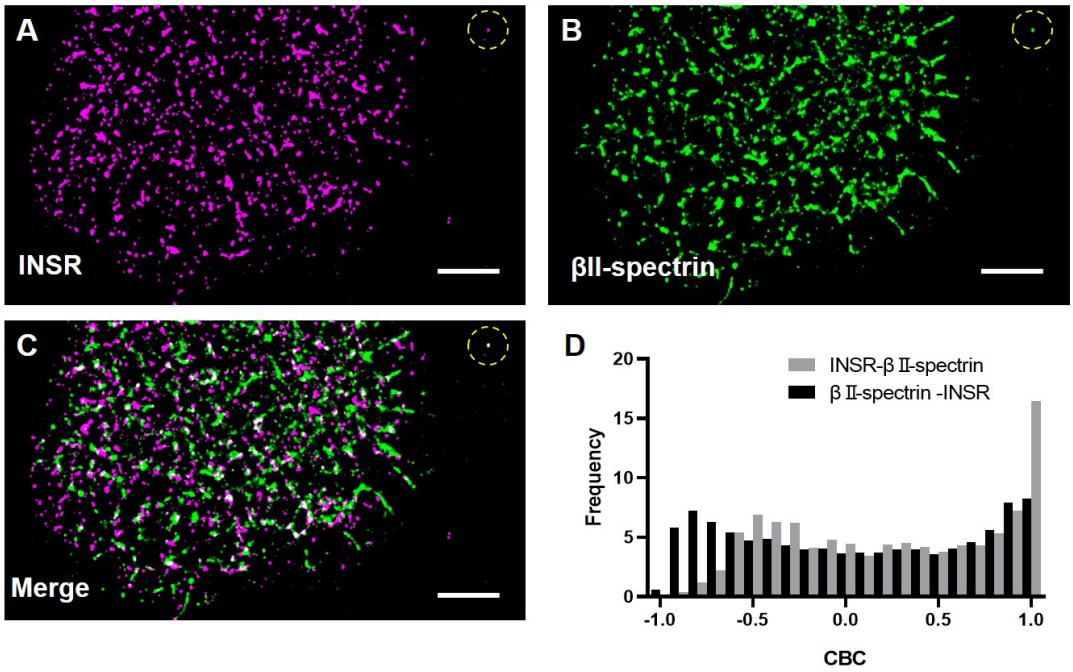

Figure S9. Spatial relationship between INSR and βII-spectrin. A-C, Two-color dSTORM images of INSR (magenta) and βII-spectrin (green) on cell membrane. Scale bars, 4 μm. D, Histogram of colocalization parameter for INSR and βII-spectrin by CBC analysis. Gray shows the distribution of CBC parameters for INSR to βII-spectrin, and Black shows βII-spectrin to INSR.